Polymer Journal (2023) 55:717–722
https://doi.org/10.1038/s41428-023-00765-w

NOTE

Preparation of crystalline polyimide nanofibers via solution crystallization

Shota Kumano[1] · Tomoyasu Takaki[1] · Tetsuya Uchida[1]

Received: 28 November 2022 / Revised: 23 January 2023 / Accepted: 23 January 2023 / Published online: 17 February 2023

Abstract

Two crystalline polyimide nanofibers (PINFs) with different morphologies were prepared. The crystalline unit cells of the aromatic PI crystals and the crystal morphologies of the fabricated PINFs were examined. PINF-I (lengths = 305 ± 152 nm and diameters = 12 ± 2 nm) was crystallized from crystalline PI dissolved in a concentrated sulfuric acid solution. The resulting PINF-I was isolated from this solution, and it did not aggregate in water. PINF-II with diameters of 105 ± 99 nm was prepared by dispersing PINF-I in a mixed water and *t*-butanol (TBA) solution (water:TBA = 4:1), followed by freeze-drying. Then, the PINF-II was heated to enhance its crystallinity. X-ray diffraction and transmission electron microscopy studies of the heat-treated PINF-II revealed a PI crystalline unit cell [orthorhombic, $a = 1.21$ nm, $b = 0.88$ nm, and $c = 2.23$ nm (molecular chain axis direction)]. The crystal structure of the heat-treated PINF-II suggested that highly crystalline PINFs were fabricated in which the PI molecular chains were oriented along the direction of the fiber lengths.

Introduction

Aromatic polyimides (PIs) are high-performance polymers with outstanding mechanical properties, high thermal stabilities, electrical insulation, radiation resistance, and chemical resistance [1–4], owing to which they are widely employed in various applications, such as microelectronics, solar cells, aerospace materials, and gas separation membranes [5–8]. PIs are generally insoluble in organic solvents because of their rigid structures and have the disadvantage of poor moldability owing to their very high glass-transition temperatures and melting points. Thus, moldable PIs with outstanding solvent solubilities that can maintain their physical properties (e.g., mechanical properties) and heat resistance have been investigated. In particular, PIs have been developed in which a bulky substituent, bent structure, or asymmetric structure has been introduced into their main chains to impart solvent solubility [9–12].

The diameters of the nanofibers are in the nanometer range. Nanofibers are high-performance nanomaterials that exhibit large specific surface areas and oriented molecular chains within the fibers; thus, they are used for various applications such as developing high-performance filters, reinforcing composite materials, and fabricating transparent materials [13–15]. Electrospinning is widely used for fabricating nanofibers [16]; however, it requires special equipment, high voltage, and a polymer that dissolves in an organic solvent. Hence, nanofiber fabrication by electrospinning is challenging because the typical PIs are not soluble in organic solvents. Therefore, PI nanofibers (PINFs) have been prepared by using a two-step fabrication approach involving electrospinning of an organic solvent–soluble PI precursor (i.e., polyamic acid) and thermal imidization [17]. However, this approach has several working steps and is expensive. Alternatively, to improve the solubilities of PIs, bending components have been introduced into their molecular chains [18]. However, the physical properties of the resultant PINFs are significantly affected owing to the decreased molecular chain rigidity and crystallinity.

Herein, we have developed an alternative approach for fabricating nanofibers by using the crystalline rigid polymer poly(*p*-phenylene benzobisoxazole) (PBO), which dissolves

Supplementary information The online version contains supplementary material available at https://doi.org/10.1038/s41428-023-00765-w.

✉ Tetsuya Uchida
tuchida@cc.okayama-u.ac.jp

[1] Graduate School of Natural Science and Technology, Okayama University, 3-1-1 Tsushima-naka, Kita-ku, Okayama 700-8530, Japan

only in strong acids [19]; highly crystalline PBO nanofibers (PBONFs) were fabricated via self-assembly of the PBO molecular chains (crystallization) by quenching the polymer solutions.

In the present study, we investigated nanofiber fabrication with a crystalline PI that exhibited solubility in concentrated sulfuric acid and maintained the rigidity of the molecular chains by introducing bulky substituents into the main chain. Two crystalline PINFs exhibiting different morphologies (PINF-I and PINF-II) were prepared via a process similar to that for PBONF fabrication. Their crystal structures were examined by estimating the PI crystalline unit cells. A PINF-I water dispersion was prepared via solution crystallization of the crystalline PI dissolved in concentrated sulfuric acid. The PINF-I water dispersion was freeze-dried and heat-treated to obtain highly crystalline PINF, and a powder was obtained in which the PINF-I was aggregated into sheets. When *t*-butanol (TBA) was added to the PINF-I water dispersion prior to freeze-drying, PINF-II was formed after freeze-drying, in which the PINF-I had aggregated into a fibrous form. Subsequently, PINF-II was heat treated to enhance its crystallinity. X-ray diffraction (XRD) and transmission electron microscopy (TEM) analyses were performed on the heat-treated PINF-II to probe the PI crystalline unit cell. The crystallographic structure of the heat-treated PINF-II was also examined.

Experimental

Material

PI was provided by Wingo Technology (Okayama, Japan) (molecular weight calculated from the degree of polymerization of the precursor = 50,000; glass-transition temperature = 259 °C; melting point = 406 °C; and thermal expansion coefficient of the PI film = 9.0×10^{-6}/K) (Fig. 1).

Preparation of PINF-I by solution crystallization

PI was dissolved in 97 wt% sulfuric acid at a concentration of 10 wt% at 50 °C. The PI–sulfuric acid solution was added dropwise into ethanol at 0 °C to precipitate the PINF-I. Subsequently, the resultant PINF-I precipitate was separated through centrifugation, and the precipitate was washed with water until the liquid was neutral by dialysis.

Preparation of PINF-II by freeze-drying a PINF-I water dispersion

A 0.01 wt% PINF-I water dispersion was prepared via ultrasonic irradiation (2510j-MT, Branson Ultrasonics Co., CT, USA, 42 kHz, 125 W) at 25 °C for 15 min. Then, TBA was added to the PINF-I water dispersion while keeping the water-to-TBA weight ratio at 4:1. The dispersion was allowed to stand overnight in a freezer (−18 °C) before freeze-drying to produce PINF-II. Freeze-drying (FDU-1200, EYELA) was conducted at a pressure and temperature of 12 Pa and 25 °C, respectively.

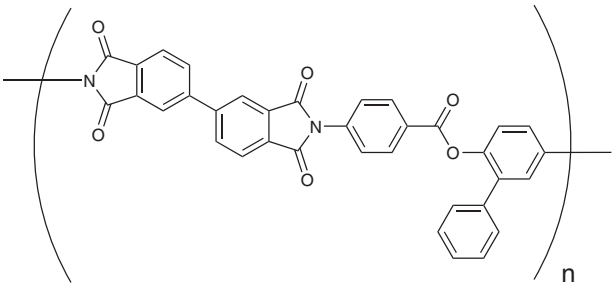

Fig. 1 Chemical structure of the polyimide (PI) used in this study

Heat treatment of PINF-II

PINF-II was heat treated under a nitrogen atmosphere at 350 °C for 1 h in an FT-101S heating furnace manufactured by Fultech Co. Ltd. (Hamamatsu, Japan).

TEM analysis

TEM (JEM 2000EXII, JEOL Co., Tokyo Japan) was used to observe the morphologies and obtain electron diffraction (ED) images of the prepared crystals. The samples for the TEM observations were prepared by placing water suspensions of the PINF-I and the heat-treated PINF-II fragments on a Cu grid with a platinum wire loop, followed by freeze-drying.

Scanning electron microscopy (SEM)

SEM was performed with a scanning electron microscope (JSM-IT100, JEOL Co. Tokyo, Japan) to observe the morphologies of PINF-II before and after the heat treatment, and an accelerating voltage of 10 kV was used. The samples were Au-coated before performing the SEM studies.

XRD measurements

XRD profiles of the PINFs were obtained with a Mini-Flex600 from Rigaku Co. (Tokyo, Japan).

Results and discussion

The representative TEM image and ED pattern for PINF-I are shown in Fig. 2a, b, respectively. The observed

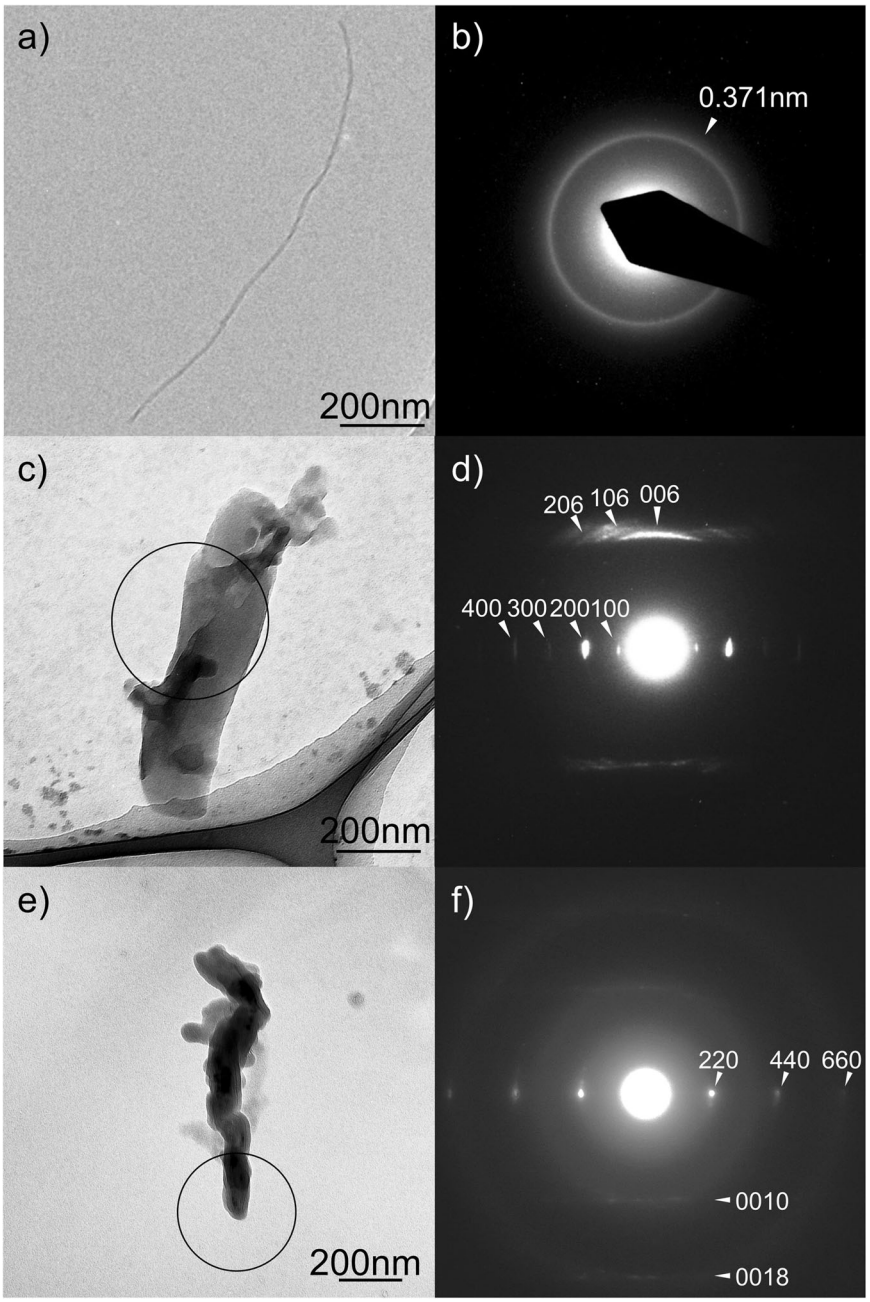

Fig. 2 Representative transmission electron microscopy (TEM) image and electron diffraction (ED) pattern obtained for the PI nanofibers (PINFs). **a** TEM image for PINF-I, **b** ED pattern for aggregated PINF-I, **c** TEM image for the heat-treated PINF-II fragment, **d** ED pattern for the circled area in **c**, **e**. TEM image of another heat-treated PINF-II fragment, and **f** ED pattern for the circled area of **e**

diameters and lengths of the prepared PINF-I were 12 ± 2 nm and 305 ± 152 nm, respectively. After preparation, the PINF-I was isolated and was stable in water without aggregation. Furthermore, the ED pattern showed a crystalline reflection for a relatively sharp ring. Thus, we confirmed the production and isolation of the crystalline nanofibers.

Highly crystalline PINFs were prepared via the following steps. PINF-I was obtained as a water dispersion. The PINF-I must be dried to perform heat treatments and improve its crystallinity. Accordingly, we analyzed drying of the PINF-I. A powder in which the PINF-I was aggregated into sheets was obtained when the PINF-I water dispersion was freeze-dried, as illustrated in Fig. S1 (see the supporting information). A dried nanofiber sample was produced while maintaining the fine fiber structure by performing freeze-drying with a mixed solvent containing water and TBA [20]. Thus, adding TBA to the PINF-I water dispersion prior to freeze-drying induced PINF-II formation, in which the PINF-I was aggregated into a fibrous form, as illustrated in Fig. 3a. The resulting fibrous PINF-II had diameters of 105 ± 99 nm in the network. The structural organization of the PINF-II is discussed at the end of the Results and Discussion section. The

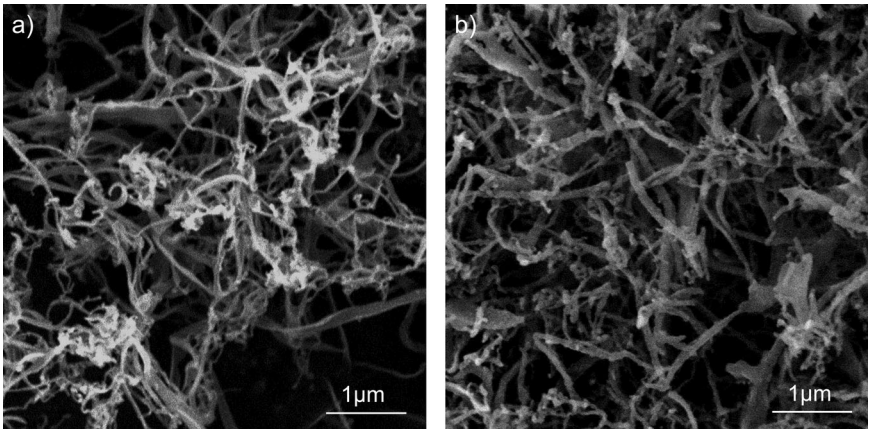

Fig. 3 Representative scanning electron microscopy images of **a** untreated and **b** heat-treated PINF-II samples

morphology of the heat-treated PINF-II was similar to that of the as-prepared PINF-II (Fig. 3b); thus, the heat treatment did not change the morphology of PINF-II. The XRD profiles of the untreated and heat-treated PINF-II are shown in Fig. 4a, b, respectively, which suggest that the heat treatment enhanced the crystallinity. In the thermogravimetry and differential thermal analysis results obtained for the heat-treated and untreated PINF-II, the endothermic peak at approximately 324 °C was removed by the heat treatment (SI Fig. S2). Hence, the unstable amorphous and disordered crystalline regions were melt-recrystallized during the heat treatment, which probably resulted in enhanced crystallinity. The approximated crystalline parameters for the orthorhombic unit cell were $a = 1.21$ nm, $b = 0.88$ nm and $c = 2.23$ nm (molecular chain axis direction), based on the XRD profiles, and the length of the PI repeating unit was 2.28 nm.

TEM images of the heat-treated PINF-II were obtained to probe the crystallographic unit cells. For the TEM analyses, fragments of the heat-treated PINF-II were prepared by cleaving the long and entangled network. The PINF-II was then cut by irradiating a water dispersion of the heat-treated PINF-II with ultrasonic waves for 30 min. Representative TEM images and ED patterns for the heat-treated PINF-II fragments are shown in Fig. 2c–f. Figure 2c shows a fiber fragment of the heat-treated PINF-II. In the ED pattern therein (Fig. 2d), the h00 reflections were perpendicular to the lengths of the fiber fragments, whereas the 00l reflections were parallel to the lengths of the fiber fragments. Thus, the crystal *a*-axis was perpendicular to the longitudinal direction of the fiber fragment, and the crystal *c*-axis corresponded to the longitudinal direction. Additionally, the crystal *a*- and *c*-axes were perpendicular to each other. Furthermore, the PI molecular chains were oriented along the lengths of the fibers. Moreover, another fragment of the heat-treated PINF-II was observed, as shown in Fig. 2e. Based on the ED pattern (Fig. 2f), the hk0 reflection was observed in the direction perpendicular to the lengths of the fiber fragments, and the 00l reflection was observed in the longitudinal direction. Thus, the [110] direction corresponded to a direction perpendicular to the longitudinal direction of the fiber fragment, whereas the crystal *c*-axis corresponded to the longitudinal direction. Moreover, the crystal *b*- and *c*-axes and the crystal *a*- and *b*-axes were orthogonal. The observed and calculated *d*-spacings of the fragments in the heat-treated PINF-II (Fig. 2d, f) are summarized in Table 1. The XRD and TEM results showed that the PI crystalline unit cell and corresponding parameters are as follows: $a = 1.21$ nm, $b = 0.88$ nm, $c = 2.23$ nm (molecular chain axis direction), orthorhombic. Furthermore, the PI molecular chains were oriented along the lengths of the PINF-II. Additionally, the PI molecular chain length calculated from the molecular weight was ca. 200 nm, but the widths of the PINF-I were only ca. 10 nm, indicating that the rigid PI molecular chains were oriented along the PINF-I length direction. These results show that freeze-drying PINF-I in a water–TBA solvent mixture led to aggregation of the PINF-I to form PINF-II. In the resulting PINF-II, PINF-I was oriented along the length direction of the PINF-II. During the subsequent heat treatment, the unstable amorphous and disordered crystalline regions were melt recrystallized, resulting in highly crystalline PI nanofibers.

Conclusion

Herein, the nanofiber fabrication methods established for the rigid polymer PBO were applied to rigid crystalline PI, and PI nanofibers were fabricated. Hence, PINF-I (diameters = 12 ± 2 nm and lengths = 305 ± 152 nm) was prepared via solution crystallization of crystalline PI dissolved in concentrated sulfuric acid. PINF-II with diameters of 105 ± 99 nm was prepared by dispersing the PINF-I in a mixed solution of water and TBA, followed by freeze-

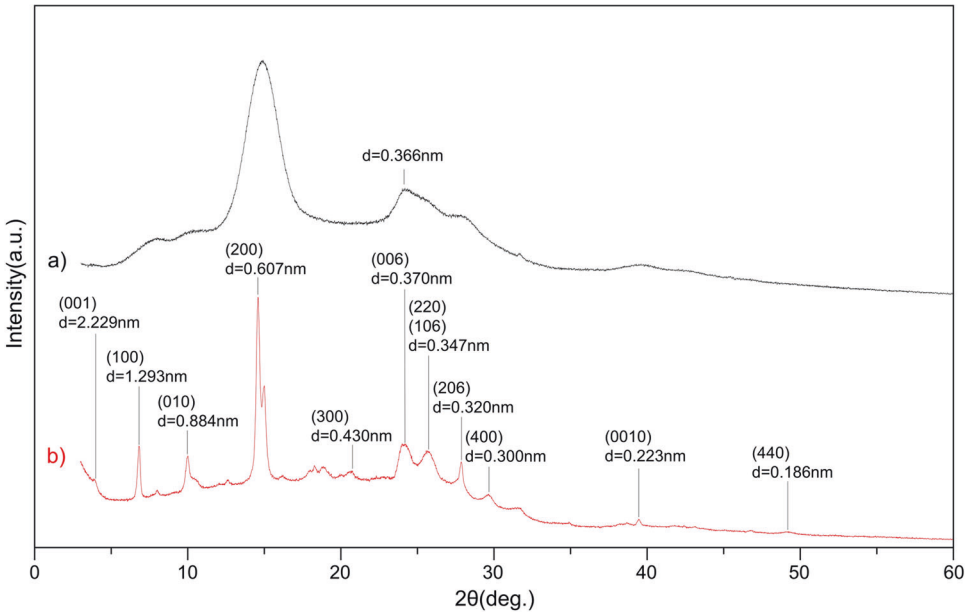

Fig. 4 X-ray diffraction profiles of **a** untreated and **b** heat-treated PINF-II samples

Table 1 Observed and calculated electron diffraction (ED) d-spacings for fragments of the heat-treated PINF-II (Fig. 2d, f)

hkl	$d_{Cal.}$(nm)	$d_{Obs.}$(nm)
100	1.214	1.194
200	0.607	0.607
300	0.405	0.429
400	0.304	0.310
006	0.372	0.387
106	0.355	0.364
206	0.317	0.320
220	0.357	0.355
440	0.179	0.176
660	0.122	0.119
0010	0.223	0.218
0018	0.124	0.127

drying. Crystallinity was improved by heat-treating the PINF-II. The XRD and TEM results obtained for the heat-treated PINF-II suggested that the PI crystalline unit cell parameters were orthorhombic, $a = 1.21$ nm, $b = 0.88$ nm, and $c = 2.23$ nm (molecular chain axis direction).

An analysis of the crystallographic structure of the heat-treated PINF-II revealed the following: (1) In the highly crystalline PINF-II, the PI molecular chains were oriented along the fiber axis. (2) Nanofiber fabrication methods used for the rigid crystalline polymer PBO can be applied to the rigid crystalline PI polymer. (3) Nanofibers can be prepared via solution crystallization of rigid crystalline polymers. These results suggest that a rigid crystalline polymer can be fabricated into nanofibers via solution crystallization.

Acknowledgements The authors are grateful to Wingo Technology for providing the polyimide samples. This work was supported by the Japanese Society for the Promotion of Science KAKENHI, grant number 22K05240.

Funding Open access funding provided by Okayama University.

Compliance with ethical standards

Conflict of interest The authors declare no competing interests.

Publisher's note Springer Nature remains neutral with regard to jurisdictional claims in published maps and institutional affiliations.

References

1. Bell VL, Stump BL, Gager H. Polyimide structure-property relationships II polymers from isomeric diamines. J Polym Sci Pol Chem. 1976;14:2275–91.
2. Volksen W, Miller RD, Dubois G. Low dielectric constant materials. Chem Rev. 2010;110:56–110.
3. Sazanov YN. Applied significance of polyimides. Russ J Appl Chem. 2001;74:1253–69.
4. Zhang M, Niu H, Wu D. Polyimide fibers with high strength and high modulus: preparation, structures, properties, and applications. Macromol Rapid Commun. 2018;39:1800141.

5. Ebnalwaled AA, Yousef A, Gerges MK, Thabet A. Synthesis of nano-polyimide for microelectronic applications. J Appl Chem Sci. 2016;6:18–30.
6. Koo D, Jung S, Seo J, Jeong G, Choi Y, Lee J, et al. Flexible organic solar cells over 15% efficiency with polyimide-integrated graphene electrodes. Joule. 2020;4:1021–34.
7. Gouzman I, Grossman E, Verker R, Astar N, Bolker A, Eliaz N. Advances in polyimide-based materials for space applications. Adv Matter. 2019;31:1807738.
8. Liu Z, Liu Y, Qiu WL, Koros WJ. Molecularly engineered 6fda-based polyimide membranes for sour natural gas separation. Angew Chem Int Ed. 2020;59:14877–83.
9. Mehdipour-Ataei S, Akbarian-Feizi L. Soluble polyimides from a semi-aliphatic diamine containing ester, amide and ether groups. Chin J Polym Sci. 2011;29:93–100.
10. Yi L, Huang W, Yan DY. Polyimides with side groups: synthesis and effects of side groups on their properties. J Polym Sci Part A Polym Chem. 2017;55:533–59.
11. Yu XH, Zhao XG, Liu CW, Bai ZW, Wang DM, Dang GD, et al. Synthesis and properties of thermoplastic polyimides with ether and ketone moieties. J Polym Sci Part A Polym Chem. 2010;48:2878–84.
12. Ghosh A, Sen SK, Banerjee S, Voit B. Solubility improvements in aromatic polyimides by macromolecular engineering. RSC Adv. 2012;2:5900–26.
13. Guibo Y, Qing Z, Yahong Z, Yin Y, Yumin Y. The electrospun polyamide 6 nanofiber membranes used as high-efficiency filter materials: filtration potential, thermal treatment, and their continuous production. J Appl Polym Sci. 2013;128:1061–9.
14. Nogi M, Iwamoto S, Nakagaito AN, Yano H. Optically transparent nanofiber paper. Adv Mater. 2009;21:1595–8.
15. Zucchelli A, Focarete ML, Gualandi C, Ramakrishna S. Electrospun nanofibers for enhancing structural performance of composite materials. Polym Adv Technol. 2011;22:339–49.
16. Subbiah T, Bhat GS, Tock RW, Parameswaran S, Ramkumar SS. Electrospinning of nanofibers. J Appl Polym Sci. 2005;96:557–69.
17. Lv YY, Wu J, Wan LS, Xu ZK. Novel porphyrinated polyimide nanofibers by electrospinning. J Phys Chem C. 2008;112:10609–15.
18. Qi HR, Zhang Y, Zhi XX, Qi L, Wu H, Wei XY, et al. Preparation and properties of electrospun polyimide ultrafine fibrous mats with excellent heat-fusibility via hot-press procedure from organo-soluble polyimides containing phenolphthalein units. Fibers Polym. 2022;23:37–47.
19. Uchida T, Furukawa M. Preparation and properties of rigid PBO polymer nanofibers prepared via crystallization from a dilute solution in sulfuric acid. J Photopolym Sci Technol. 2014;27:177–80.
20. Borisova A, Bruyn MD, Budarin VL, Shuttleworth PS, Dodson JR, Segatto ML, et al. A sustainable freeze-drying route to porous polysaccharides with tailored hierarchical meso- and macroporosity. Macromol Rapid Commun. 2015;36:774–9.